Cost Feasibility Analysis of Translucent Optical Networks With Shared Wavelength Converters

Oscar Pedrola, Davide Careglio, Miroslaw Klinkowski, Josep Solé-Pareta, and Keren Bergman

***Abstract*—Translucent optical networks have emerged as potential yet feasible candidates to bridge the gap between the opaque and transparent network architectures. By allowing electrical 3R signal regeneration only at selected points in the network, translucent architectures represent a cost-effective, power-efficient solution. Concurrently, forecasts predicting highly dynamic traffic patterns make it crucial for next-generation transport networks to engage highly agile technologies that include sub-wavelength switching (SWS). In translucent SWS networks, contention resolution is achieved through the still technologically immature all-optical wavelength converters (WCs). Since WCs are expected to be expensive, power-consuming devices, there has been significant research effort on devising WC-sharing architectures, which aim at minimizing the number of these devices in the network. WC sharing, however, requires complex switching fabrics that involve a much higher number of optical gates and stronger degradation due to physical layer impairments (more electrical 3R regenerators). It is clear, then, that the technological interest of WC-sharing architectures mainly depends on the cost trade-offs existing between these three components. For this reason, in this work, we carry out a comprehensive cost feasibility analysis of translucent networks based on asynchronous WC-sharing packet switches. After modeling a set of translucent WC-sharing switching fabrics, we assess their performance in an isolated node scenario in terms of the number of WCs and optical gates required. Given the results obtained, we select the shared-per-node (SPN) architecture to compare its hardware requirements with those of a network based on dedicated WC nodes (i.e., one WC per wavelength and input port). To this end, an iterative simulation algorithm is used to dimension translucent SWS networks considering a broad range of continental-scale topologies. The results are first analyzed using relative cost values, and finally the viability/feasibility of WC-sharing schemes is discussed considering state-of-the-art technology. Our main conclusion is that, for SPN-based architectures to become cost effective, the cost of WCs has to be at least two orders of magnitude higher than that of the optical gate and similar to or lower than that of the electrical 3R regenerator.**

***Index Terms*—Cost analysis; Regenerator; Sub-wavelength switching; Wavelength converter.**

Manuscript received August 28, 2012; revised November 12, 2012; accepted November 25, 2012; published December 6, 2013 (Doc. ID 175142).

Oscar Pedrola (e-mail: opedrola@ac.upc.edu) is with the Advanced Broadband Communications Center (CCABA), Universitat Politècnica de Catalunya (UPC), Barcelona, Spain, and is also with the Department of Electrical Engineering, Columbia University, New York, New York 10027, USA.

Davide Careglio and Josep Solé-Pareta are with the Advanced Broadband Communications Center (CCABA), Universitat Politècnica de Catalunya (UPC), Barcelona, Spain.

Miroslaw Klinkowski is with the National Institute of Telecommunications, 1 Szachowa Str., Warsaw, Poland.

Keren Bergman is with the Department of Electrical Engineering, Columbia University, New York, New York 10027, USA.

Digital Object Identifier 10.1364/JOCN.5.000001

I. Introduction

Over the last years, optical transport networks (OTNs) have been undergoing an architectural evolution from traditional *opaque* toward *transparent* architectures. The two main driving forces behind this re-definition are, on the one hand, network operators' aim to lower both capital and operational expenditures (CAPEX/OPEX), and, on the other, several key optical technology breakthroughs, which provided relevant improvements in the main optical signal functions and boosted the implementation of integrated transmission and switching sub-systems at the physical layer [1].

To provide the required quality of transmission (QoT), current opaque architectures rely on electrical 3R (re-timing, re-shaping and re-amplification) regeneration at every node [2]. However, considering both the ultra-fast pace at which traffic is growing, and the fact that the impact of regeneration strongly depends on several data transmission parameters such as the line rate and the modulation format, it is clear that the opaque concept poses serious scalability problems regarding, among other things, heat dissipation, power consumption, physical space, and costs [1,3]. These issues triggered the evolution toward transparent networks, which, undoubtedly, represent a conceptually ideal approach for next-generation OTNs. However, transparency is not yet achievable, as the immaturity of all-optical 3R regeneration leaves no means to properly mitigate the strong signal degradation induced by physical layer impairments (PLIs) [4]. Indeed, despite the fact that all-optical 3R regeneration has been and is the focus of intensive research (see, e.g., [5–9]), it is not yet a practical solution [10].

As a matter of fact, novel optical systems and devices allowing for longer transmission distances, higher bit rates, and more closely spaced wavelength channels have dramatically increased the sensitivity to PLIs, which accumulate and severely limit optical reach [11]. To go beyond this, optical reach is therefore necessary for the optical signal to undergo electrical 3R regeneration. This scenario has positioned the *translucent* architecture as a potential yet feasible intermediate step to continue moving forward in the evolution [4,12]. In a translucent infrastructure not all nodes are regenerator locations but only a subset of them, thereby leading to a cost-effective, power-efficient network model, which is very attractive to network operators[3].

The design of a translucent network entails a careful engineering of the so-called routing and regeneration placement (RRP) problem, which, in order to meet a target QoT network

1943-0620/13/020001-12/$15.00

performance, strategically locates regenerators in the network. In order to estimate the PLI impact, these algorithms require the definition of a QoT estimator and a pre-specified minimum signal QoT performance (QoT_{th}), below which the signal is considered beyond the receiver's sensitivity [13]. In the context of wavelength switched optical networks (WSONs), RRP has been the focus of intensive research over the last years (see, e.g., [12,14–17]), and has eventually led to standardization activities within IETF [18].

Concurrently, forecasts predicting traffic scenarios featuring short-lived, small granularity flows make it crucial for next-generation OTNs to engage highly agile optical transport technologies that include sub-wavelength switching (SWS) (see, e.g., [19,20]). By leveraging recent advances in nanosecond-range photonic devices such as fast tunable lasers and fast switching elements, optical packet/burst/flow switching (OPS/OBS/OFS) technologies have emerged as potential alternatives to today's power-consuming router architectures. Indeed, future OTNs supporting dynamic SWS can realize high throughput and highly flexible networks providing finer payload granularities and high bandwidth efficiency [21].

The architectures and solutions discussed and evaluated in this work can be applied to any SWS paradigm. Therefore, without loss of generality, we use the terms *SWS* and *packet* generically to refer, respectively, to the switching paradigm under which the OTN is operating and the optical data unit of such an infrastructure (i.e., packets/bursts/flows). Similarly, we use the term *regenerator* to refer to the electrical 3R regenerator (i.e., optical–electrical–optical conversion).

In SWS networks, however, the classical RRP algorithms developed for wavelength-routed networks are not applicable anymore, as due to their statistical multiplexing nature there exists a fair competition for accessing regenerator resources. Indeed, in such a case, RRP extends to the so-called routing and regenerator placement and dimensioning (RRPD) problem [22,23]. With the routing paths and locations of regenerators selected (RRP), the dimensioning phase (D) is responsible for obtaining the minimum amount of such regenerators so as to meet a pre-defined target QoT network performance. To deal with PLIs in SWS networks, in [22] we modeled a translucent SWS fabric configured following the tune-and-select scheme (see Fig. 1). This photonic switch is based on semiconductor optical amplifier (SOA) technology to ensure the provisioning of high-speed all-optical switching in an asynchronous fashion. Given the lack of optical buffers, in this architecture, contention resolution is achieved through all-optical wavelength converters (WCs) [24,25]. As shown in Fig. 1, a dedicated full-range fixed-input, tunable-output wavelength converter (FITO-WC) is available for each wavelength and input port. Furthermore, PLIs in the network are mitigated by equipping, according to RRPD decisions, some of the nodes with a limited size pool of regenerators. This pool consists of a set of R fixed receivers, an electrical buffering stage and a set of R lasers emitting at pre-defined wavelengths (i.e., $\lambda_1,\ldots,\lambda_R$). Since the output signal of a FITO-WC is handled by the SWS node controller, fairness in the access to the regenerator pool can be achieved. Here, fairness means that any packet entering the regenerator pool may access any regenerator, and thus there exists a fair competition for the use of regenerators. Note that this feature has important

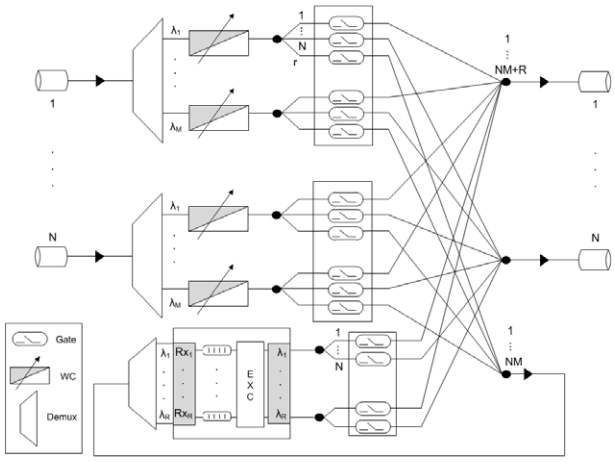

Fig. 1. Translucent SWS node with dedicated WCs (DWCs) [23]. FITO-WCs are used.

implications during the network planning stage, as it allows for a significant simplification of the RRPD problem [23].

However, full-range wavelength tunability results in very complex, power-consuming and lossy WC devices [26–28]. Indeed, current techniques to achieve conversion between any given combination of input/output wavelengths involve cascading a set of limited range WCs, thereby leading to very expensive devices [29]. For these very reasons, there has been significant research effort to devise photonic switch architectures which exploit WC sharing [30], and, by this means, minimize the number of WCs required to meet a target loss performance. In these node architectures, packet loss is not only caused by the lack of a free wavelength at the selected output port, but also due to the lack of a free WC. The most well-known instance is the shared-per-node (SPN) configuration [30], which represents the perfect sharing scheme, as a pool of WCs is fairly shared among all wavelengths from all input ports. In SPN, WCs are required to be tunable-input, tunable-output WCs (TITO-WCs), which are assumed to be the most complex and expensive type of WC [31]. TITO-WCs are also used in the shared-per-link (SPL) architecture [32], in which a bank of WCs is dedicated to each output fiber. SPL, however, is not considered in this work as it suffers from inefficient WC sharing, particularly under unbalanced traffic conditions [32,33]. More recently, in [31,33], two alternative WC-sharing configurations were proposed that use less complex WCs, specifically the shared-per-input-wavelength (SPIW) and the shared-per-output-wavelength (SPOW) switching fabrics. Whilst SPIW relies on FITO-WCs as the DWC node, SPOW requires tunable-input, fixed-output WCs (TIFO-WCs), which are considered to be the less complex, and therefore cheaper, WCs [33,34].

The consideration of WC-sharing switching fabrics has nevertheless important implications on the optical signal degradation along its way from source to destination. Indeed, the higher power penalties paid at passive devices (splitters/combiners) as well as the higher number of active components (SOA gates inducing higher ASE noise levels) that the signal traverses increase the impact of PLIs, thereby limiting the size and capacity of nodes [35,36]. In addition,

stronger degradation due to PLIs shortens optical reach, and thus a network based on WC-sharing switching fabrics will require more regenerators to be deployed. Summarizing, when compared to the DWC node, WC-sharing architectures minimize the number of WCs, but at the same time require more complex switching fabrics (more optical gates) and increase the impact of PLIs (more regenerators). It is clear, then, that the interest of WC-sharing switches with respect to DWC-based architectures depends on the quality of the above mentioned cost trade-off.

For this reason, in this work, we carry out a thorough cost feasibility analysis for translucent SWS networks based on WC-sharing node architectures. To this end, we first model and assess the performance of a set of translucent WC-sharing switching fabrics and, considering a realistic node configuration for OTNs, we select one of the WC-sharing nodes to perform an adequate power-budget and noise analysis. Then, considering an optical-signal-to-noise ratio (OSNR)-based QoT model and an RRPD algorithm [22,23], a translucent SWS network based on WC-sharing nodes is equipped with the required pools of regenerators. Through simulation, we approximate the exact number of WCs that are required at each node to meet the loss performance of the DWC case. Finally, we consider relative cost values and state-of-the-art technology for optical gates, WCs and regenerators, to analyze, over a broad range of large-scale topologies, the viability of WC-sharing schemes for next-generation translucent SWS-based OTNs.

The rest of this paper is organized as follows. Section II details the translucent WC-sharing switching architectures considered in this paper and surveys the most relevant works. In addition, a performance analysis of a series of candidate WC-sharing switching fabrics is carried out. Section III details the process considered to dimension a translucent SWS network based on WC-sharing architectures. Afterwards, in Section IV, we first analyze the networks' CAPEX by using relative cost values for the main components, and second we discuss the feasibility of WC-sharing schemes by considering an experimental all-optical WC design and commercially available devices. Finally, Section V concludes the paper.

II. Translucent WC-Sharing Architectures

We assume photonic switches with N input/output mono-fiber links that each carry M wavelength channels (i.e., $\lambda_1 \ldots \lambda_M$) and perform asynchronous packet switching. Figure 2, depicts the SPN switching fabric including a pool of R regenerators that is used to mitigate the impact of PLIs. Since in these schemes WCs are a scarce resource, an initial splitting stage, which consists of a bank of high-speed switching SOA gates, can transfer the signal either directly to the selected output fiber (if no wavelength conversion is needed) or to a bank of C TITO-WCs, which is perfectly shared among all wavelengths from all input ports. After wavelength conversion is performed, a second SOA gating stage grants access to either the selected output port or the pool of regenerators. It is worth noticing that, thanks to the tunability of the output wavelength at WCs, a fair access to the regenerator pool is also provided with this architecture.

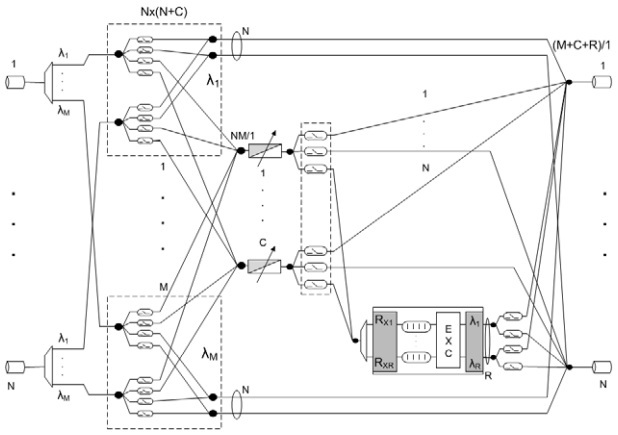

Fig. 2. Translucent shared-per-node (SPN) architecture. TITO-WCs are used.

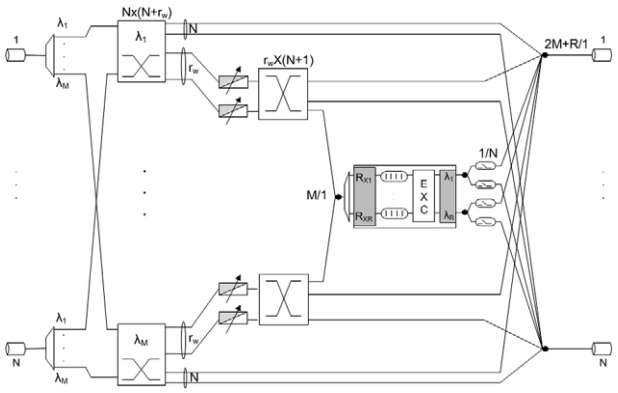

Fig. 3. Translucent shared-per-input-wavelength (SPIW) architecture. FITO-WCs are used.

In an attempt to improve the trade-off proposed by the SPN scheme, research focused on WC-sharing schemes that could use simpler, less expensive WCs. In [31,33], the authors present the SPIW (also known as shared-per-wavelength (SPW)) and SPOW architectures.

Figure 3 presents the translucent SPIW switch. In this case, WCs are arranged in small banks of size r_w and dedicated to each input wavelength. Hence, if there is a packet arriving at λ_1 requiring wavelength conversion, whatever the input port is, it will only have access to the bank of WCs dedicated to λ_1. Again, thanks to the output wavelength tunability of the WC device in SPIW, a common pool of regenerators can be fairly shared. Note that, for both SPIW and SPOW (see Fig. 4), the space switching stages follow the same SOA-based structure as shown in Fig. 2 for the SPN node.

Finally, Fig. 4 illustrates the SPOW switching fabric, where WCs are arranged in small banks of size r_w, one per output wavelength. In this case, however, since the less expensive TIFO-WCs are used, the WC output is fixed to a different wavelength in each bank. In SPOW, an arriving packet at λ_1 has more chances to find a free WC than in the SPIW configuration, as it can try any bank of WCs except for the one

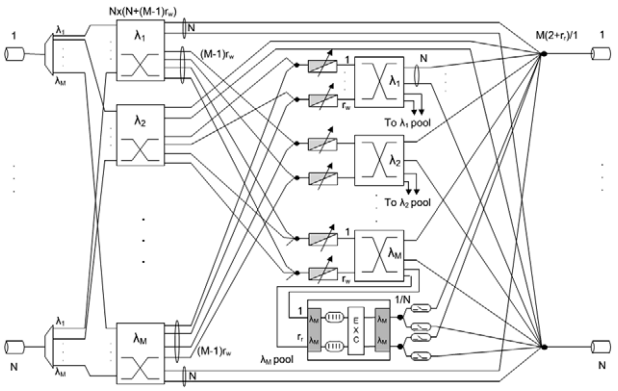

Fig. 4. Translucent shared-per-output-wavelength (SPOW) architecture. TIFO-WCs are used.

where the output wavelength is set to λ_1. As to the regenerator pool configuration, and in order to maximize the sharing of regenerators, it has to be arranged in small banks, each consisting of a set of r_r regenerators for the same wavelength (fixed by the output of each FITO-WC). Finally, the complexity of the presented translucent node architectures in terms of the number of both WCs and SOA gates is reported in Table I.

The efficiency in minimizing the number of WCs required to meet a target loss performance of these switching fabrics has been extensively studied under both synchronous and asynchronous scenarios, balanced and unbalanced traffic, and mono/multi-fiber schemes (see, e.g., [30–33,37] and references therein). As discussed in the last section, in order to carry out the cost comparison between the DWC and WC-sharing architectures, in this work we focus on a mono-fiber, asynchronous scenario. To this end, our next objective is to select one of the WC-sharing architectures presented to continue with the cost study. In [33], a loss performance analysis is carried out under asynchronous operation, and it is shown that SPOW can provide WC savings (in terms of the number of devices required) very close to those obtained by SPN while slightly increasing the number of SOA gates. Note, however, that SPOW WCs are TIFO, and hence less expensive. The evaluation is nevertheless conducted considering $N = 16$ and 32, numbers that are too high for core networks, which are our objective in this paper. Indeed, in realistic backbone networks such as the ones considered in this paper (see Appendix A for details), the highest node degree (N) is rather small, typically around 4 [38,39] (5 in our instances).

Under these circumstances, and assuming Poisson traffic arrivals, we expect the arrangement of WCs in small banks in both SPIW and SPOW to have a serious adverse effect on the packet loss performance, which may lead to inefficient WC sharing. Another drawback of the SPOW scheme that must be mentioned is the fact that regenerators are also arranged in small banks. Given the Erlang-based dimensioning function used in RRPD [22], which favors the grouping of regenerators, the SPOW set-up is highly likely to require a higher number of regenerators to meet a given target loss performance in the access to these pools.

A. WC-Sharing Architecture Evaluation in an Isolated Node

To analyze the performance of the different schemes, we conduct a series of simulations considering an isolated node with $N = 2$ and 5, that is, the two extreme values for a typical node degree in core OTNs (see Appendix A for more simulation details). In addition, for this experiment we neglect the impact of PLIs, and hence no regenerators are considered (i.e., $R, r_r = 0$). We analyze the packet loss probability (PLP) as a function of the wavelength conversion ratio (ψ), which is equal to $\frac{\mathscr{C}}{NM}(\mathscr{C} = 0 \ldots NM)$ for SPN, and $\frac{r_w}{N}(r_w = 0 \ldots N)$ for SPIW and SPOW. We note that the scheduling algorithms considered in this work are the ones described in [33].

Figures 5(a) and 5(b) provide the results obtained, respectively, for the $N = 2$ and $N = 5$ nodes. In Fig. 5(a), we consider three different load (ρ) values (i.e., 0.4, 0.5 and 0.8) for the SPN and DWC nodes. As expected, SPN at lower loads requires fewer WCs (lower ψ) to meet the performance of the DWC node. We also simulate SPIW and SPOW for the intermediate load case ($\rho = 0.5$). In the $N = 2$ node, only three possible ψ values exist for SPIW and SPOW (i.e., 0, 0.5 and 1). One can observe the poor performance of SPIW, and that SPOW requires as many WCs as DWC to meet the target performance, thus not providing any WC reduction. In Fig. 5(b), where $\rho = 0.5$ is assumed, whilst the higher value of N, enabling more ψ values in both SPIW and SPOW, allows the latter to slightly improve its performance, SPIW still results in a very inefficient scheme. Approximately, $\psi = 0.675$ and 1 for SPN and SPOW in the $N = 2$ node and 0.5 and 0.8 for the $N = 5$ node. Using these values, the hardware requirements for these architectures are reported in Table II. Although SPOW uses WCs that are expected to be cheaper, in comparison to SPN it requires more WCs and a significantly higher number of SOA gates.

TABLE I
NUMBER OF WCS AND SOA GATES REQUIRED IN THE TRANSLUCENT DWC, SPN, SPIW AND SPOW ARCHITECTURES

Scheme	Device	Quantity
DWC	FITO-WCs	$N \cdot M$
	SOA gates	$N \cdot M \cdot (N+1) + R \cdot N$
SPN	TITO-WCs	C
	SOA gates	$M \cdot N \cdot (N+C) + C \cdot (N+1) + R \cdot N$
SPIW	FITO-WCs	$M \cdot r_w$
	SOA gates	$M \cdot N \cdot (N+r_w) + M \cdot r_w \cdot (N+1) + R \cdot N$
SPOW	TIFO-WCs	$M \cdot r_w$
	SOA gates	$M \cdot N \cdot (N+r_w \cdot (M-1)) + M \cdot r_w \cdot (N+r_r) + M \cdot r_r \cdot N$

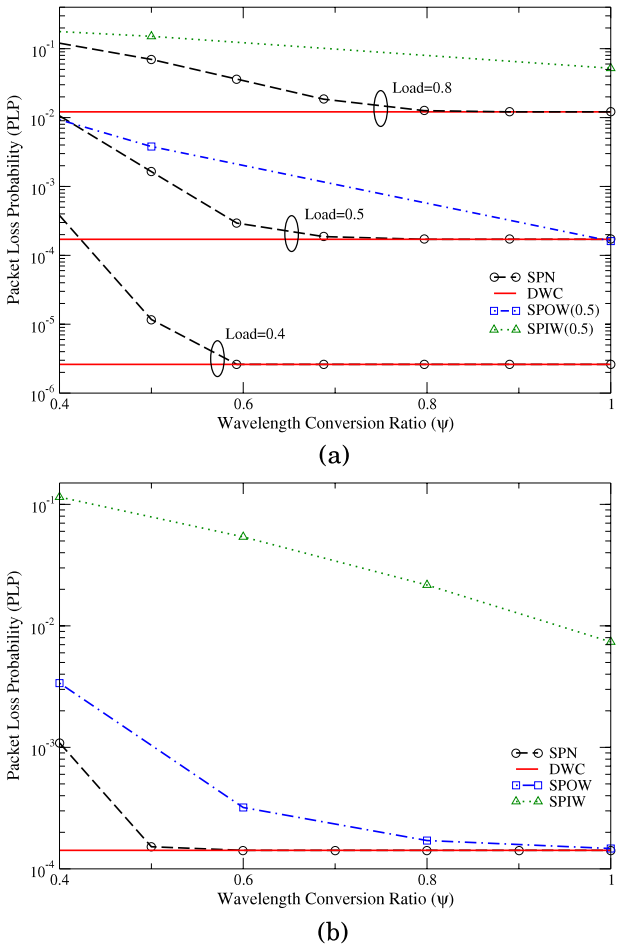

Fig. 5. (Color online) Performance evaluation of the different WC-sharing architectures proposed in an isolated node. Packet loss probability as a function of the wavelength conversion ratio with (a) $N = 2$, (b) $N = 5$. $M = 32$ wavelengths per link each at 10 Gbps.

TABLE II
NUMBER OF WCS AND SOA GATES REQUIRED IN AN ISOLATED NODE CONFIGURED AS DWC, SPN AND SPOW SWITCH

Scheme	N	WCs	SOA gates
DWC	2	64	192
	5	160	960
SPN	2	44	3076
	5	80	14,080
SPOW	2	64 ($r_w = 2$)	4224
	5	128 ($r_w = 4$)	21,280

Taking into account these results and the fact that the average node degree in core OTNs is much closer to 2 than 5 (see Appendix A), we believe the SPN architecture is the best candidate to conduct the cost feasibility analysis for translucent OTNs based on WC sharing. Finally, it is important to notice that incoming packets requiring regeneration (i.e., access to the regenerator pool) will require the use of a WC, as regenerators are accessed through the bank of WCs. Hence, nodes equipped with regenerators (translucent nodes) will require an increase of ψ in order to meet the target loss performance. This issue, however, will be analyzed in more detail in the next section.

III. TRANSLUCENT SWS NETWORK DESIGN

To design the translucent SWS network we follow the approach presented in [22,23]. Specifically, we first consider a QoT model based on the off-line estimation of the OSNR contributions of both nodes and links in the end-to-end signal path. Hence, in this work we refer to the system QoT_{th} as OSNR_{th}. We also point out that there may exist strong signal degradation due to inaccuracies in these estimations, non-linear impairments arising from the high-speed ON–OFF switching nature of the traffic as well as those introduced by WC operation and amplifier dynamics [40]. Due to these non-desirable impacts, it is necessary to consider a penalty margin (e.g., 2 dB extra) when determining an adequate OSNR_{th} [41].

A. Power-Budget and Noise Analysis

In order to adequately tune and set up the components building both the DWC and SPN nodes, we consider the characteristic path that an optical signal follows between two neighboring nodes (see Fig. 6). We can anticipate that SPN, due to the more complex configuration, will suffer from higher PLI impact.

First, we set the power constraints to −16 dBm/channel (set by link losses) at the input (input of the erbium doped fiber amplifier (EDFA) pre-amplifier), and to 0 dBm/channel at the output (output of the EDFA booster amplifier). All the components considered are currently commercially available. For the EDFA (pre/inline/booster) specifications, we refer the reader to [22]. We model an all-optical WC considering a block consisting of a fast tunable laser and a non-linear WC-type SOA. Optical gates are based on high-speed SOA switches. The specifications for these devices are provided in Table III. In order to compensate splitting losses, we tune the gains for the different amplifiers making sure the power constraints of each component are respected. As detailed in [22], at this point, we can obtain, for a DWC-based network, the set of paths ($\mathcal{Q}$) that require regeneration at some point (i.e., whose OSNR level at the receiving end is below OSNR_{th}), and thus that are input to the RRPD algorithm. In SPN, however, we must first obtain the number of WCs C that are available at each node in order to compute the actual splitting and coupling losses in the node. In the next section, this issue is tackled by means of an iterative simulation algorithm.

B. Translucent SPN Network Dimensioning

It is obvious that the key issue when dimensioning the SPN network is to find out the minimum number of WCs required (per node) so that the performance of the DWC architecture is matched. To approximate the exact number of WCs required at each node, we implement an iterative algorithm based on

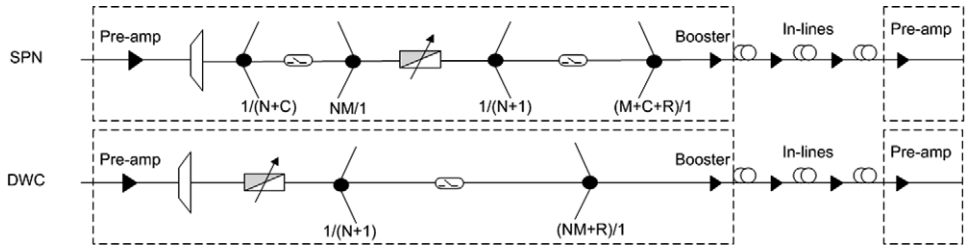

Fig. 6. Characteristic signal path between two translucent SWS nodes configured either as DWC or SPN.

TABLE III
COMPONENT SPECIFICATIONS CONSIDERED

Span length	65 km
Fiber attenuation	0.2 dB/km + 3 dB (cable margin)
Quantum noise	−58 dBm
WDM demux	insertion loss ≈ 5.5 dB
Fast tunable laser	
Manufacturer	Finisar
Model	S7500 [42]
Operating range	Full C-band (89 chan.)
Channel spacing	50 GHz
Switching time	<150 ns
WC-type SOA	
Manufacturer	CIP Technologies
Model	SOA-XN-C-14-FCA [43]
Noise figure	6.5 dB
Typ. gain	25 dB
Sat. output power	12 dBm
Recovery time	10 ps
SOA switch	
Manufacturer	Thorlabs
Model	SOA1013S [44]
Noise figure	9.5 dB
Max. gain	10 dB
Sat. output power	12 dBm
Switching speed	<1 ns

network simulation. The pseudo-code is shown in Procedure 1. We denote the set of nodes in the network as $\mathcal{V}$ and the set of nodes equipped with regenerators (translucent nodes) as $\mathcal{H} \subseteq \mathcal{V}$.

As explained in Section II, this analysis is dependent on the network load assumed (ρ), and hence this is an input parameter to be taken into account. Procedure 1 first runs a simulation considering an opaque network (i.e., no PLI impact) using the DWC switch in order to obtain the target PLP for each node of the network. Then, the loop between lines 4 and l3 is responsible for obtaining the minimum number of WCs (C_v, $\forall v \in \mathcal{V}$) that ensures that each node in the SPN network matches the performance of its DWC counterpart. Next, the power-budget and noise analysis is performed and the set of paths $\mathcal{Q}$ is obtained. Using $\mathcal{Q}$, the RRPD algorithm is run and the required regenerator pools are deployed across the network. Note that RRPD requires as parameter the target loss performance in the access to these pools (B^{QoT}). As previously mentioned, however, the fact that regenerator pools lie behind the shared bank of WCs leads to degraded loss performance in translucent nodes. For this reason, these nodes will require more WCs to meet the target DWC performance. To this end, between lines l6 and 25, the algorithm runs a second loop until the target PLP for every node is achieved. Note that, since routing paths are computed at the very beginning of the algorithm and do not vary, this second loop does not affect the WC requirements at nodes $v \notin \mathcal{H}$. PLP values are obtained by averaging 10 independent runs of the simulation. Each run lasts enough simulation steps so that very accurate values are obtained (i.e., reporting negligible confidence intervals). Once Procedure 1 finishes, we have available the total number of WCs, regenerators and SOA switches required by the translucent SWS network based on SPN switching fabrics.

Procedure 1 Translucent SPN network dimensioning

INPUT: $\mathcal{V}$, ρ;
OUTPUT: Translucent SPN network dimensioned;
1: $C_v = 0, \forall v \in \mathcal{V}$;
2: Simulate-network(DWC, ρ);
3: Obtain $PLP(v,$ DWC$), \forall v \in \mathcal{V}$;
4: **repeat**
5: Simulate-network(SPN, ρ);
6: **for all** node $v \in \mathcal{V}$ **do**
7: **if** $PLP(v,$ SPN$) > PLP(v,$ DWC$)$ **then**
8: $C_v \leftarrow C_v + 1$;
9: **else**
10: Node v meets target $PLP(v,$ DWC$)$;
11: **end if**
12: **end for**
13: **until** all node $v \in \mathcal{V}$ meet target $PLP(v,$ DWC$)$
14: Perform power-budget and noise analysis and obtain $\mathcal{Q}$;
15: Run RRPD($\mathcal{Q}$, ρ, B^{QoT});
16: **repeat**
17: Simulate-network(SPN, ρ);
18: **for all** node $v \in \mathcal{H}$ **do**
19: **if** $PLP(v,$ SPN$) > PLP(v,$ DWC$)$ **then**
20: $C_v \leftarrow C_v + 1$;
21: **else**
22: Node v meets target $PLP(v,$ DWC$)$;
23: **end if**
24: **end for**
25: **until** all node $v \in \mathcal{H}$ meet target $PLP(v,$ DWC$)$

In the next section, we dimension each of the translucent topologies considering both the DWC and SPN architectures, and finally, using relative cost values and current state-of-the-art technology for WCs, SOA gates and regenerators, we analyze the viability of deploying future SWS OTNs based on WC-sharing architectures.

TABLE IV
NETWORK SIMULATION SETUP

Network	ρ	PLP_{opaque}	B^{QoT}	DWC WCs
Core	0.45	$2.64\cdot10^{-3}$	$5\cdot10^{-4}$	1472
Basic	0.27	$2.88\cdot10^{-3}$	$5\cdot10^{-4}$	2624
Usa–Can	0.2	$9.71\cdot10^{-4}$	$1\cdot10^{-4}$	3904
Large	0.125	$1.35\cdot10^{-3}$	$1\cdot10^{-4}$	3744

IV. COST COMPARISON OF TRANSLUCENT SWS NETWORKS BASED ON DWC AND SPN PHOTONIC SWITCHES

In this section, in order to analyze the cost implications of the SPN switching fabric and compare it against the DWC one, we dimension four translucent SWS-network topologies (see Appendix A) following the approach presented in Section III. Note that for the DWC network it is enough to first use the OSNR model to obtain the set of paths requiring regeneration, and second execute an RRPD algorithm to deploy regenerators. It should be mentioned that the aim of the RRPD formulation is to minimize the number of regenerators deployed in the network whilst, at the same time, guaranteeing that losses caused by QoT signal degradation (optical signals whose OSNR is below $OSNR_{th}$) are kept well below those caused by contentions in network links. Hence, once dimensioned, a translucent network must show an overall PLP similar to that of an opaque network, where PLIs are perfectly mitigated.

Taking these details into account, in Table IV, we report the simulation scenario for each of the network topologies. Since the typical operation range for SWS networks is for overall PLPs of the order of 10^{-3} and lower, we select for each network a load value (ρ) which could be considered as a worst-case scenario network dimensioning. These loads allow us to obtain the PLP of the opaque network (PLP_{opaque}), which is the target PLP performance to be met by the translucent networks. Since PLP_{opaque} in both the Usa–Can and Large networks is slightly lower, we also reduce the maximum contention allowed in the access to regenerator pools (B^{QoT}). Finally, for illustration purposes, the number of WCs required in the DWC network are also provided in Table IV. Note that the number of WCs in a DWC network corresponds to the number of regenerators used in an opaque network (i.e., one per channel and input port).

Using the OSNR model detailed in Section III, and assuming an $OSNR_{th}$ = 21 dB (2 dB penalty [23]), we show in Fig. 7 the percentage of paths that require regeneration at some intermediate node for both the DWC and SPN architectures. We consider the optical end-to-end paths of the four continental-scale network topologies provided in Appendix A. Routing paths are obtained using the optimization approach detailed in [23]. One can observe the higher PLI impact in SPN, a fact which will increase the number of regenerators required to meet the target QoT. These paths are therefore the input data required to run an RRPD algorithm, which will be responsible for deciding regenerator pool locations and their size. To solve RRPD, in this analysis we make use of the load-based mixed integer linear programing (LB-MILP) formulation proposed in [23].

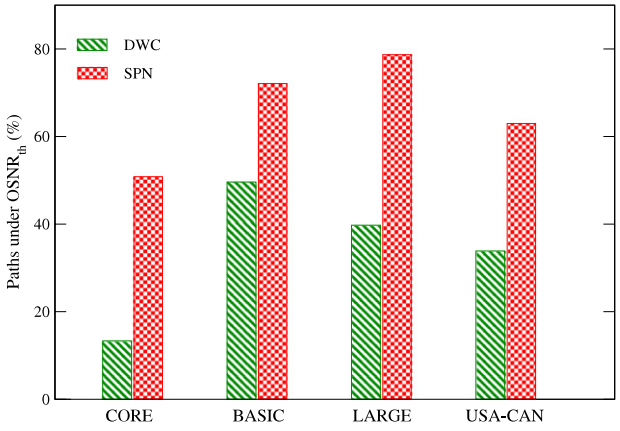

Fig. 7. (Color online) Percentage of end-to-end optical paths that do not meet the OSNR requirements for both the DWC and SPN architectures.

LB-MILP is a two-step MILP formulation which focuses on grouping regenerators in as few nodes as possible in order to minimize regenerator locations/sites and the overall network load requiring regeneration.

Figures 8(a) and 8(b) provide the difference in hardware requirements between the translucent SPN and DWC networks. As expected, Fig. 8(a) reports the significant gain (improving with network size) in terms of the number of WCs that can be achieved with the SPN switch, and that this improvement comes at the expense of an increase in the number of regenerators to compensate the higher degradation due to PLIs. However, we can also note in Fig. 8(b) that, due to the more complex switching fabric, SPN requires a much larger number of optical SOA gates, a fact which inevitably leads to a substantial increase in both hardware cost and power consumption.

To analyze the feasibility of the SPN node, we now consider relative cost values for the WCs (C_{WC}), SOA gates (C_{Gate}) and regenerators (C_{3R}), and compute the network CAPEX considering the complexity formulas presented in Table I. Since the two architectures use different WCs, we define the cost of a WC in the SPN network as $C_{WC-SPN} = \gamma C_{WC-DWC}$, where γ is defined as

$$\gamma = \frac{C_{TITO-WC}}{C_{FITO-WC}}. \tag{1}$$

Finally, we define the following two relative parameters to analyze the results of both network scenarios.

$$\alpha = \frac{C_{WC}}{C_{Gate}}, \tag{2}$$

$$\beta = \frac{C_{3R}}{C_{WC}}. \tag{3}$$

Figure 9, provides the results for the four network topologies. The y-axis represents the cost difference (as a percentage) between the SWC and DWC networks. Hence, negative y-axis values mean that SPN results in a cheaper network. This cost

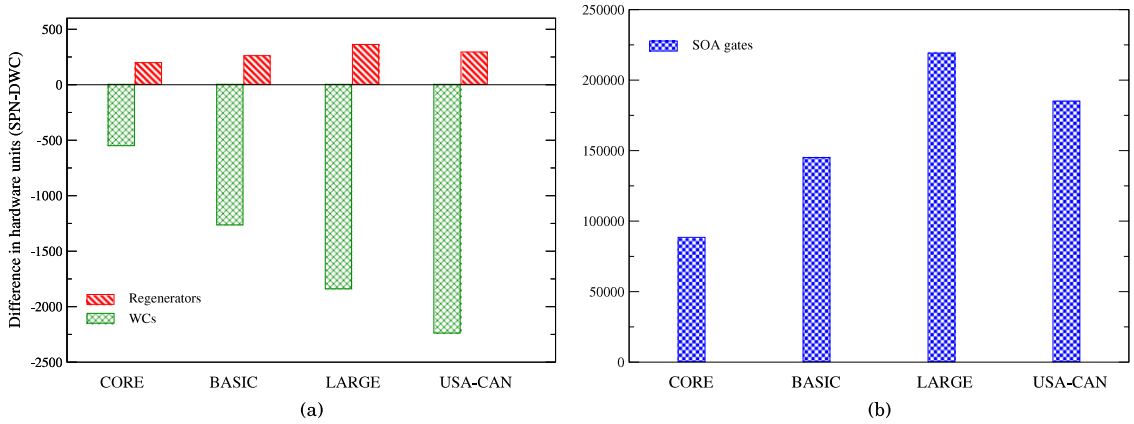

Fig. 8. (Color online) Hardware requirement difference between the SPN and DWC network architectures in terms of (a) WCs and regenerators and (b) SOA gates. Note that negative values mean SPN requires fewer units than DWC.

is evaluated as a function of β, which deals with the relative cost difference between WCs and regenerators. The curves in the plots represent four different values for α considering $\gamma = 1$, that is, that the WCs of both architectures have the same cost. In addition, an additional curve is shown to illustrate the effect of assuming a 10% (γ = 1.1) cost difference between the two WCs for $\alpha = 200$.

Considering γ = 1, one can observe that, for the SPN network to become cost-effective, on the one hand α has to be at least 200 in the smaller networks (Core, Basic), slightly more than 100 in the Large, and 100 for Usa–Can. Thus, SPN requires two orders of magnitude difference between a WC and a gate. This is a clear consequence of the much larger number of SOA gates required in SPN. Also, the benefits of SPN improve with network size, as more nodes allow for larger reductions in the number of WCs in the network. On the other hand, we can also observe that, on increasing β, the network cost becomes dominated by $C_{\text{Regen.}}$. Since SPN requires more regenerators than DWC to mitigate PLIs, it will require β to be as low as possible. To be precise, considering $\alpha = 200$, we can estimate that, for SPN to improve upon DWC, β should be ≤1 in both the Core and Basic networks and approximately ≤2 and 5, respectively, in the Large and Usa–Can topologies. Furthermore, we can notice that, if a relatively small γ exists (e.g., 10–15%), SPN will only turn out to be beneficial in large networks (e.g., Large, Usa–Can).

We have now analyzed the cost implications of the SPN switching fabric by using relative values for the different devices, and discussed the values of α, β and γ where SPN results in a cost-effective network architecture. We devote the next section to discussing and forecasting the feasibility of these results by considering state-of-the-art components and their respective market prices.

A. SPN Outlook Using State-of-the-art Components

In order to assess the feasibility of the SPN architecture, we first estimate the costs of the three main elements considering commercially available devices. Note that we only take into consideration the main components, and that the additional electronic circuitry required is not accounted for.

To begin with, the cost of a commercially available high-speed SOA switch is around $C_{\text{Gate}} = \$1685$ [44]. To model the regenerator, and according to the architecture proposed in Section II, we consider tunable 10 Gbps transceivers (see, e.g., [45,46]) based on mature technology, which provides both the optical–electrical (O–E) and electrical–optical (E–O) stages. The cost of these 10 Gbps transceivers is around C_{3R} = \$6k. It should be mentioned, however, that the cost for such device increases to more than \$20k for 40 Gbps [47]. Finally, to model the WC, we consider the experimental design presented in [48], where a two-stage monolithically integrated all-optical WC is shown to be able to provide TITO operation at 10 Gbps. The main components of this WC are (a) two sampled-grating distributed Bragg reflector (SG-DBR) tunable lasers [49], (b) four non-linear SOAs [43] (two for a parallel cross-gain modulated (XGM) SOA structure, and two for a SOA-based Mach–Zehnder interferometer (SOA–MZI), which relies on cross-phase modulation (XPM)), and (c) three SOA booster amplifiers [50] that are placed at the output of the two SG-DBR lasers for amplification and power balancing purposes. An estimation of the current market price for all these devices is around C_{WC} = \$16k. However, given both the difficulty in creating the control circuitry to operate these devices at high speed, and the challenge of integrating these components into a single stand-alone sub-system to be used in OTNs, we envisage the cost of a future all-optical TITO WC to be substantially higher.

According to these estimations, it seems possible to motivate the region of interest for β values, where the cost of a regenerator is similar to or lower than the cost of a WC. Although 3R regenerators are power consuming (with high impact on OPEX costs), WCs requiring such complex designs involving various processes such as XPM and XGM are also expected to consume a significant amount of power [26]. Furthermore, experimental WC designs have shown interesting 2R capabilities, which in the future are expected to improve optical reach, and as a result expand the transparent network regions without employing re-timing processes [51]. For the α region, that is, values of α that make SPN attractive from the cost point of view, we have estimated a difference of around an order of magnitude. However, we

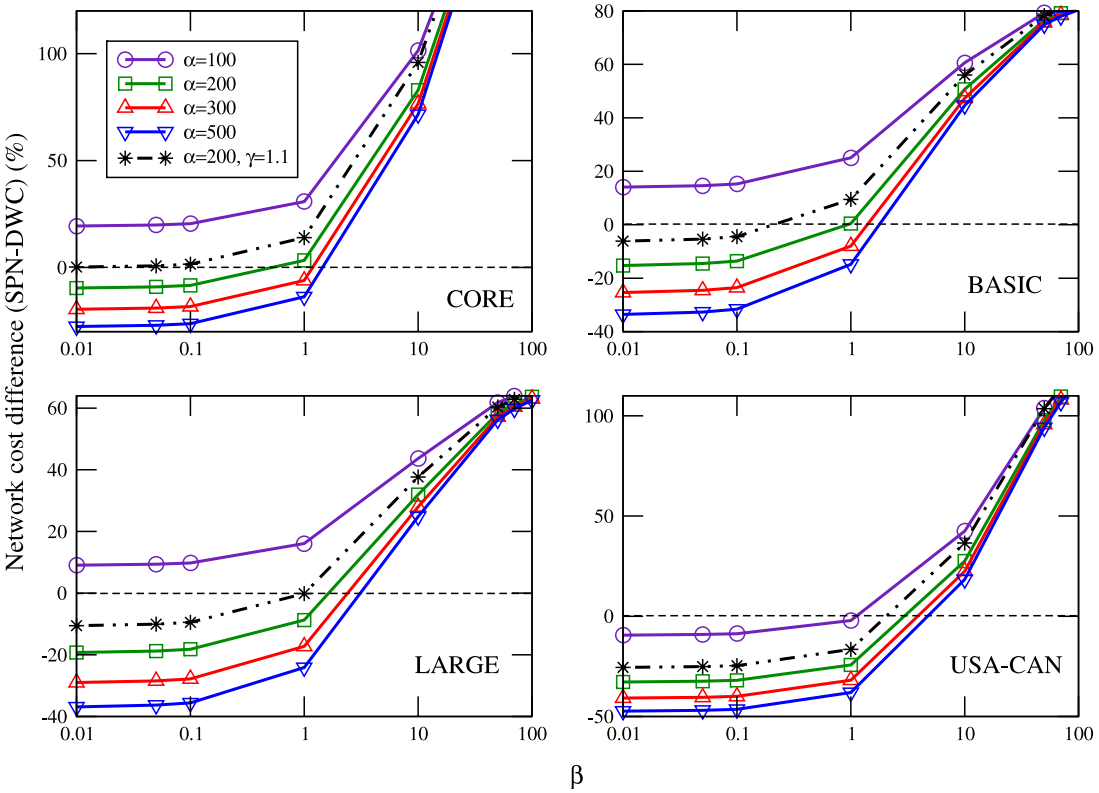

Fig. 9. (Color online) Cost difference between the SPN and DWC translucent networks as a function of α and β. Parameter γ is fixed to 1 except for one curve, where it is set to 1.1. Note that negative values mean that SPN results in a less expensive network.

have found that at least two are required between the gate and WC cost. In favor of SPN, we have two facts: (1) the optical gate is already a technologically mature device; (2) the number of gates required in the SPN network is more than two orders of magnitude higher than the number of WCs (e.g., in the Large network 237,377 gates vs. 1905 WCs). Whilst (1) can foster mass production of gates, (2) may lead to substantial discounts due to bulk purchasing, and therefore we may envisage future scenarios where the requirements for α are fulfilled. Finally, regarding γ, it must be mentioned that the cost difference between TITO and FITO WCs will depend on the technology considered to implement the WC [52], and that we have observed that only small percentages could be afforded in large size networks.

Summarizing, given the more complex architecture, and hence higher number of SOA gates, it is crucial for the success of WC-sharing architectures that the cost and power consumption of all-optical WCs is as high as possible in comparison to that of the gates. Although in this study we have focused on CAPEX costs (i.e., power consumption has not been analyzed), our findings are in line with those presented in [26], where the authors compare the power consumption of DWC and WC-sharing nodes and conclude that, for WC-sharing architectures to consume less energy than DWC, WCs have to be high energy consuming devices. All in all, we believe this study allows us to predict a bleak future for the deployment of OTNs based on WC-sharing architectures.

V. Conclusions

This paper addressed the feasibility of deploying future translucent SWS OTNs based on WC-sharing photonic switches. To this end, we have first modeled a set of translucent WC-sharing node architectures by equipping nodes with limited size pools of electrical 3R regenerators. Assuming an isolated node scenario, we have assessed the performance of these candidate switches and found that the SPN switching fabric is the most appropriate for core transport networks. Afterwards, we performed a comprehensive cost feasibility study of translucent SWS networks based on SPN switches. For this purpose, we compared its hardware requirements (WCs, optical gates and electrical 3R regenerators) with those of a network with dedicated WCs (DWC), that is, one WC is available per wavelength and input port. Using an iterative simulation algorithm, we have dimensioned a set of continental-scale translucent SWS networks using both SPN and DWC nodes. To analyze the cost of these networks, we have first used relative costs for the main components, and finally discussed the feasibility of deploying WC-sharing switches by using state-of-the-art components. The main conclusion is that, for translucent networks based on WC-sharing switches to become cost-effective, the cost of a WC has to be at least two orders of magnitude higher than that of the optical gate, and similar to or lower than that of an electrical 3R regenerator. Although the study presented has been performed under the assumption of a core network framework, which

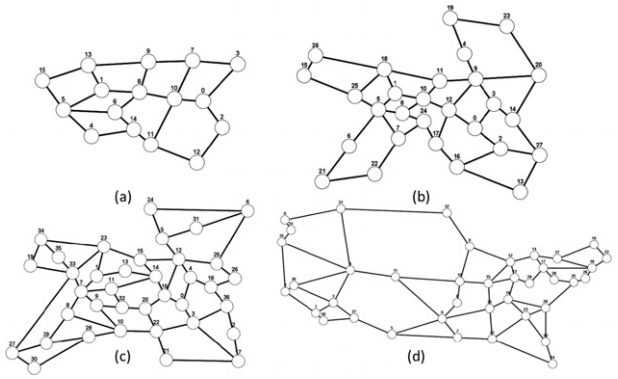

Fig. 10. (a) Core (2.875), (b) Basic (2.92), (c) Large (3.08), (d) Usa–Can (3.128).

nowadays is focusing more on the deployment of 40–100 Gb/s coherent detection transmission systems, the results can be extrapolated to a more appropriate scenario for SWS like the *metro* network case. The metro network consideration would impact, on the one hand, on the average link length (which is shorter), thereby reducing (or even eliminating) regeneration requirements. On the other, the average node degree would probably be higher, and thus the choice of the WC-sharing architecture could differ from the one we made in this paper (i.e., SPN). However, the main issue to overcome by WC-sharing architectures would be the same, that is, that the savings in terms of the number of WCs achieved through WC sharing are clearly offset by the huge increase in the number of optical gates required to perform the switching operation.

Appendix A: Simulation Scenario

In our simulation scenario, we consider several topologies (see Fig. 10): a set of Pan-European [53] networks known as Large (a), Basic (b) and Core (c), with 37, 28 and 16 nodes and 57, 41 and 23 links respectively, and the JANOS-US-CA [54] (d), a reference network that interconnects cities in the USA and Canada with 39 nodes and 61 links. In the figure caption, the average node degree for each of the networks is reported.

Network links are bidirectional and dimensioned with the same number of wavelengths $M = 32$. The transmission bit rate is set to 10 Gbps for both transmitters at edge nodes and regenerators at core nodes. We assume that each node is both an edge and a core bufferless node capable of generating packets destined to any other nodes. For the sake of simplicity, the switching and processing times are neglected. The traffic is uniformly distributed between nodes. We assume that each edge node offers the same amount of traffic to the network; this offered traffic is normalized to the transmission bit rate. Packets are generated according to a Poisson arrival process and have exponentially distributed lengths. The mean packet duration is 100 μs (1 Mb). Since we consider Poisson arrivals and a constant load, changing the packet size would imply either reducing or increasing inter-arrival times, and hence the packet size does not have any impact on the PLP results obtained [55].

All simulations have been conducted on the JAVOBS [56] sub-wavelength network simulator on an Intel Core 2 Quad 2.67 GHz with 4 GB RAM. We use CPLEX (version 12.1) [57] as the underlying MILP-solver for the LB-MILP algorithm.

Acknowledgments

The research leading to these results has received funding from the European Community's Seventh Framework Programme FP7/2007-2013 under grant agreement 247674 (STRONGEST Project), the Spanish Ministry of Science through the FPU Program and the DOMINO Project (TEC2010-18522). It was also supported in part by the NSF Engineering Research Center for Integrated Access Networks (CIAN) (sub-award Y503160). This paper was presented in part at NOC 2011 [58].

O. Pedrola would also like to thank Lynn West and her team from the Wisconsin State Laboratory of Hygiene (WSLH) for the interesting discussions held during the preparation of this manuscript.

References

[1] S. Sygletos, I. Tomkos, and J. Leuthold, "Technological challenges on the road toward transparent networking," *J. Opt. Netw., OSA*, vol. 7, no. 4, pp. 321–350, Apr. 2008.

[2] G. Ellinas, J.-F. Labourdette, S. Chaudhuri, J. Walker, E. Goldstein, K. Bala, S. Chaudhuri, and L. Lin, "Network control and management challenges in opaque networks utilizing transparent optical switches," *IEEE Commun. Mag.*, vol. 42, no. 2, pp. 16–24, Feb. 2004.

[3] J. Solé-Pareta, S. Subramaniam, D. Careglio, and S. Spadaro, "Cross-layer approaches for planning and operating impairment-aware optical networks," in *Proc. of the IEEE, Special Issue on The Evolution of Optical Networks*, no. 5, May 2012, vol. 100, pp. 1118–1129.

[4] B. Ramamurthy, H. Feng, D. Datta, J. Heritage, and B. Mukherjee, "Transparent vs. opaque vs. translucent wavelength-routed optical networks," in *Optical Fiber Communication Conf., 1999, and the Int. Conf. on Integrated Optics and Optical Fiber Communication. OFC/IOOC '99. Technical Digest*, 1999, vol. 1, pp. 59–61.

[5] Y. Huang, X. Lei, I. Glesk, V. Baby, L. Bin, and P. Prucnal, "Simultaneous all-optical 3R regeneration of multiple WDM channels," in *Lasers & Electro Optics Society 18th Ann. Meeting, IEEE LEOS 2005*, Oct. 2005, pp. 59–61.

[6] M. Rochette, J. L. Blows, and B. J. Eggleton, "3R optical regeneration: An all-optical solution with BER improvement," *Opt. Express*, vol. 14, no. 14, pp. 6414–6427, July 2006.

[7] S. J. Ben Yoo, "All-optical regeneration for ultra-long fiber links and its prospects for future applications with new modulation formats," in *Optical Fiber Communication (OFC), collocated National Fiber Optic Engineers Conf., 2009 Conf. on (OFC/NFOEC)*, Mar. 2009, OThS4.

[8] M. Funabashi, Z. Zhu, B. Pan, Z. Xiang, S. J. B. Yoo, D. L. Harris, and L. Paraschis, "First field demonstrations of 1000-hop cascaded all-optical 3R regeneration in 10 Gb/s NRZ transmission," in *Conf. on Lasers and Electro-Optics (CLEO), OSA*, 2006. Q1

[9] T. Kise, K. N. Nguyen, J. M. Garcia, H. N. Poulsen, and D. J. Blumenthal, "Cascadability properties of MZI-SOA-based all-optical 3R regenerators for RZ-DPSK signals," *Opt. Express*, vol. 19, no. 10, pp. 9330–9335, Apr. 2011.

[10] S. Azodolmolky, M. Klinkowski, E. Marín-Tordera, D. Careglio, J. Solé-Pareta, and I. Tomkos, "A survey on physical layer impairments aware routing and wavelength assignment algorithms in optical networks," *J. Comput. Netw.*, vol. 53, no. 7, pp. 926–944, May 2009.

[11] C. V. Saradhi and S. Subramaniam, "Physical layer impairment aware routing (PLIAR) in WDM optical networks: issues and challenges," *IEEE Commun. Surv. Tutorials*, vol. 11, no. 4, pp. 109–130, Dec. 2009.

[12] G. Shen and R. S. Tucker, "Translucent optical networks: the way forward [topics in optical communications]," *IEEE Commun. Mag.*, vol. 45, no. 2, pp. 48–54, Feb. 2007.

[13] B. Lavigne, F. Leplingard, L. Lorcy, E. Balmefrezol, J. Antona, T. Zami, and D. Bayart, "Method for the determination of a quality-of-transmission estimator along the lightpaths of partially transparent networks," in *33th European Conf. on Optical Communication, 2007. ECOC '07*, 2007, vol. 3, pp. 287–8.

[14] X. Yang and B. Ramamurthy, "Sparse regeneration in translucent wavelength-routed optical networks: Architecture, network design and wavelength routing," *J. Photonic Network Commun.*, vol. 10, pp. 39–53, 2005.

[15] W. Zhang, J. Tang, K. Nygard, and C. Wang, "REPARE: Regenerator placement and routing establishment in translucent networks," in *IEEE Int. Conf. on Global Commun. (GLOBECOM 2009)*, Dec. 2009.

[16] R. Muñoz, R. Martínez, and R. Casellas, "Challenges for GMPLS lightpath provisioning in transparent optical networks: wavelength constraints in routing and signalling," *IEEE Commun. Mag.*, vol. 47, no. 8, pp. 26–34, Aug. 2009.

[17] K. Manousakis, P. Kokkinos, K. Christodoulopoulos, and E. Varvarigos, "Joint online routing, wavelength assignment and regenerator allocation in translucent optical networks," *J. Lightwave Technol.*, vol. 28, no. 8, pp. 1152–1163, Apr. 2010.

[18] Y. Lee, G. Bernstein, D. Li, and G. Martinelli, A framework for the control of wavelength switched optical networks (WSON) with impairments. IETF draft, 2010 [Online]. Available: http://tools.ietf.org/html/draft-ietf-ccamp-wson-impairments-08.

[19] S. J. Ben Yoo, "Optical packet and burst switching technologies for the future photonic internet," *J. Lightwave Technol.*, vol. 24, no. 12, pp. 4468–92, 2006.

[20] V. Chan, "Optical flow switching," in *Optical Fiber Communication (OFC), collocated National Fiber Optic Engineers Conf., 2010 Conf. on (OFC/NFOEC)*, Mar. 2010, OWI6.

[21] C. P. Lai, A. Shacham, and K. Bergman, "Demonstration of asynchronous operation of a multiwavelength optical packet-switched fabric," *IEEE Photon. Technol. Lett.*, vol. 22, no. 16, pp. 1223–25, Aug. 2010.

[22] O. Pedrola, D. Careglio, M. Klinkowski, and J. Solé-Pareta, "Offline routing and regenerator placement and dimensioning for translucent OBS networks," *J. Opt. Commun. Netw.*, vol. 3, no. 9, pp. 651–666, Sept. 2011.

[23] O. Pedrola, D. Careglio, M. Klinkowski, and J. Solé-Pareta, "Regenerator placement strategies for translucent OBS networks," *J. Lightwave Technol.*, vol. 29, no. 22, pp. 3408–3420, Nov. 2011.

[24] S. L. Danielsen, P. Hansen, and K. E. Stubkjaer, "Wavelength conversion in optical packet switching," *J. Lightwave Technol.*, vol. 16, no. 9, pp. 2095–2108, Dec. 1998.

[25] J. M. H. Elmirghani and H. T. Mouftah, "All-optical wavelength conversion: technologies and applications in DWDM networks," *IEEE Commun. Mag.*, vol. 38, no. 3, pp. 86–92, Dec. 2000.

[26] V. Eramo and M. Listanti, "Power consumption in bufferless optical packet switches in SOA technology," *J. Opt. Commun. Netw.*, vol. 1, no. 3, pp. B15–B29, Aug. 2009.

[27] D. Apostolopoulos, D. Klonidis, P. Zakynthinos, K. Vyrsokinos, N. Pleros, I. Tomkos, and H. Avramopoulos, "Cascadability performance evaluation of a new NRZ SOA–MZI wavelength converter," *IEEE Photon. Technol. Lett.*, vol. 21, no. 18, pp. 1341–1343, Sept. 2009.

[28] M. Spyropoulou, N. Pleros, K. Vyrsokinos, D. Apostolopoulos, M. Bougioukos, D. Petrantonakis, A. Miliou, and H. Avramopoulos, "40 Gb/s NRZ wavelength conversion using a differentially-biased SOA–MZI: Theory and experiment," *J. Lightwave Technol.*, vol. 29, no. 10, pp. 1489–1499, May 2011.

[29] V. Eramo, M. Listanti, and M. Spaziani, "Resource sharing in optical packet switches with limited-range wavelength converters," *J. Lightwave Technol.*, vol. 23, no. 2, pp. 671–687, Feb. 2005.

[30] V. Eramo, M. Listanti, and P. Pacifici, "A comparison study on the number of wavelength converters needed in synchronous and asynchronous all-optical switching architectures," *J. Lightwave Technol.*, vol. 21, no. 2, pp. 340–355, Feb. 2003.

[31] V. Eramo, A. Germoni, C. Raffaelli, and M. Savi, "Packet loss analysis of shared-per-wavelength multi-fiber all-optical switch with parallel scheduling," *J. Comput. Netw.*, vol. 53, no. 2, pp. 202–216, Feb. 2009.

[32] N. Akar, E. Karasan, and K. Dogan, "Wavelength converter sharing in asynchronous optical packet/burst switching: An exact blocking analysis for markovian arrivals," *IEEE J. Sel. Areas Commun.*, vol. 24, no. 12, pp. 69–80, Dec. 2006.

[33] N. Akar, C. Raffaelli, M. Savi, and E. Karasan, "Shared-per-wavelength asynchronous optical packet switching: a comparative analysis," *J. Comput. Netw.*, vol. 54, no. 13, pp. 2166–2181, Sept. 2010.

[34] Y. Fukushima, H. Harai, S. Arakawa, and M. Murata, "Design of wavelength-convertible edge nodes in wavelength-routed networks," *J. Opt. Netw.*, vol. 5, no. 3, pp. 196–209, Mar. 2006.

[35] H. Buchta and E. Patzak, "Analysis of the physical impairments on maximum size and throughput of SOA-based optical burst switching nodes," *J. Lightwave Technol.*, vol. 26, no. 16, pp. 2821–2830, Aug. 2008.

[36] C. Raffaelli, M. Savi, G. Tartarini, and D. Visani, "Physical path analysis in photonic switches with shared wavelength converters," in *12th Anniversary Int. Conf. on Transparent Optical Networks (ICTON 2010)*, June 2010, vol. 1, Mo.C1.5.

[37] C. Raffaelli, M. Savi, and A. Stavdas, "Multistage shared-per-wavelength optical packet switch: Heuristic scheduling algorithm and performance," *J. Lightwave Technol.*, vol. 27, no. 5, pp. 538–551, Mar. 2009.

[38] J. M. Simmons, "Analysis of wavelength conversion in all-optical express backbone networks," in *Optical Fiber Communication (OFC), collocated National Fiber Optic Engineers Conf., 2002 Conf. on (OFC/NFOEC)*, Mar. 2002, TuG2.

[39] O. Gerstel, R. Ramaswami, and S. Foster, "Merits of hybrid optical networking," in *Optical Fiber Communication (OFC), collocated National Fiber Optic Engineers Conf., 2002 Conf. on (OFC/NFOEC)*, Mar. 2002, TuG1.

[40] J. Junio, D. C. Kilper, and V. W. S. Chan, "Channel power excursions from single-step channel provisioning," *J. Opt. Commun. Netw.*, vol. 4, no. 9, pp. A1–A7, Sept. 2012.

[41] R. Martínez, R. Casellas, R. Munoz, and T. Tsuritani, "Experimental translucent-oriented routing for dynamic lightpath provisioning in GMPLS-enabled wavelength switched optical networks," *J. Lightwave Technol.*, vol. 28, no. 8, pp. 1241–1255, Apr. 2010.

[42] Finisar, CW tunable laser: Mod. S7500, 2012 [Online]. Available: http://www.finisar.com/products/optical-components/Tunable-Lasers/S7500.

[43] CIP-Technologies, Non-linear SOA: Mod. SOA-XN-OEC-1550, 2012 [Online]. Available: http://www.ciphotonics.com/download/datasheet/soa/SOA-XN-C-14-FCA_A.pdf.

[44] Thorlabs, High-speed SOA switch: Mod. soa1013sxs, 2012 [Online]. Available: http://www.thorlabs.us/thorProduct.cfm?partNumber=SOA1013S.

[45] Menara, Tunable OTN XFP DWDM 11.1 Gb/s transceiver with integrated G.709 and E-FEC, 2012 [Online]. Available: http://www.menaranet.com/downloads/187-04001-00_OTN_TUNABLE_XFP_10Gb.pdf.

[46] Finisar, Tunable XFP (T-XFP) transceiver, 2012 [Online]. Available: http://www.finisar.com/products/optical-modules/xfp/FTLX4213xxxxxx.

[47] Finisar, 40 Gbps-OTU3 DWDM tunable very long reach transponder, 2012 [Online]. Available: http://www.finisar.com/products/optical-modules/300-pin/53DPAAU4JBLCB.

[48] J. A. Summers, M. L. Masanovic, V. Lal, and D. J. Blumenthal, "Monolithically integrated multi-stage all-optical 10 Gbps push–pull wavelength converter," in *Optical Fiber Communication (OFC), collocated National Fiber Optic Engineers Conf., 2007 Conf. on (OFC/NFOEC)*, Mar. 2007, OthT2.

[49] JDSU, SG-DBR tunable laser source, 2012 [Online]. Available: http://www.acronymeo.com/jdsgtulaso24.html.

[50] Thorlabs, Booster SOA: Mod. boa1004s, 2012 [Online]. Available: www.thorlabs.us/thorProduct.cfm?partNumber=BOA1004S.

[51] D. Apostolopoulos, K. Vyrsokinos, P. Zakynthinos, N. Pleros, and H. Avramopoulos, "An SOA-MZI NRZ wavelength conversion scheme with enhanced 2R regeneration characteristics," *IEEE Photon. Technol. Lett.*, vol. 21, no. 19, pp. 1363–1365, Oct. 2009.

[52] V. Eramo, A. Germoni, A. Cianfrani, M. Listanti, and C. Raffaelli, "Evaluation of power consumption in low spatial complexity optical switching fabrics," *IEEE J. Sel. Top. Quantum Electron.*, vol. 17, no. 2, pp. 396–405, Mar./Apr. 2011.

[53] S. Maesschalck, D. Colle, I. Lievens, M. Pickavet, P. Demeester, C. Mauz, M. Jaeger, R. Inkret, B. Mikac, and J. Derkacz, "Pan-European optical transport networks: An availability-based comparison," *J. Photonic Network Commun.*, vol. 5, no. 3, pp. 203–225.

[54] S. Orlowski, M. Pióro, A. Tomaszewski, and R. Wessäly, "Sndlib 1.0 survivable network design library," in *Proc. INOC'07*, 2007.

[55] Z. Rosberg, H. L. Vu, M. Zukerman, and J. White, "Performance analyses of optical burst-switching networks," *IEEE J. Sel. Areas Commun.*, vol. 21, no. 7, pp. 1187–1197, Sept. 2003.

[56] O. Pedrola, S. Rumley, M. Klinkowski, D. Careglio, C. Gaumier, and J. Solé-Pareta, "JAVOBS: a flexible simulator for OBS network architectures," *Academy Publisher J. Networks*, vol. 5, no. 2, pp. 256–264, Feb. 2010.

[57] IBM, ILOG CPLEX, 2012 [Online]. Available: http://www-01.ibm.com/software/integration/optimization/cplex/.

[58] O. Pedrola, D. Careglio, M. Klinkowski, and J. Solé-Pareta, "Translucent OBS network architectures with Dedicated and Shared wavelength resources," in *2011 16th European Conf. on Networks and Optical Communications (NOC)*, July 2011.